J Fluoresc (2011) 21:1987–1996
DOI 10.1007/s10895-011-0899-y

ORIGINAL PAPER

Chemometric Analysis of Excitation Emission Matrices of Fluorescent Nanocomposites

João M. M. Leitão · Roma Tauler · Joaquim C. G. Esteves da Silva

Received: 6 November 2010 / Accepted: 9 May 2011 / Published online: 24 May 2011

Abstract The performance of multivariate curve resolution (MCR-ALS) to decompose sets of excitation emission matrices of fluorescence (EEM) of nanocomposite materials used as analytical sensors was assessed. The two fluorescent nanocomposite materials were: NH_2-polyethylene glycol (PEG200) functionalized carbon dots, sensible to aqueous Hg(II) (CD); and, CdS quantum dots attached to the dendrimer DAB, sensible to the ionic strength of the aqueous medium (CdS-DAB). The structures of these sets of EEM, obtained as function of the Hg(II) concentration and ionic strength, are characterized by collinear properties (CD) and non-linear spectral variations (CdS-DAB). MCR-ALS was able to detect that the source of the collinearities is the presence of different size CD that show similar affinity towards Hg(II). Moreover, MCR-ALS was able to model the non-linear spectral variations of the CdS-DAB that are induced by varying ionic strength. The chemometric pre-processing of the fluorescent data sets using soft-modelling multivariate curve resolution like MCR-ALS is a critical step to transform these nanocomposites with interesting fluorescent proprieties into analytical useful nanosensors.

Keywords MCR-ALS · Fluorescence excitation emission matrices · Nanocomposites · Sensors · Carbon dots · Quantum dots

J. M. M. Leitão
Centro de Investigação em Química (CIQ-UP), Grupo de Ciências Biológicas e Bioanalíticas, Faculdade de Farmácia de Coimbra, Polo das Ciências da Saúde,
3000-432 Coimbra, Portugal

R. Tauler
Department of Environmental Chemistry, IIQAB-CSIC,
Jordi Girona 18-26,
08026 Barcelona, Spain

J. C. G. E. da Silva (✉)
Centro de Investigação em Química (CIQ-UP),
Departamento de Química e Bioquímica,
Faculdade de Ciências da Universidade do Porto,
R. Campo Alegre 687,
4169-007 Porto, Portugal
e-mail: jcsilva@fc.up.pt

Introduction

One of the most promising areas of scientific research in analytical chemistry is the application of new nanomaterials to the development of new analytical methodologies [1–5]. Particularly interesting is the development of new fluorescent nanomaterials, for example quantum dots (QDs) [1–5] and carbon dots (CDs) [6–14], coupled to the great potential for the development of new bioanalytical methodologies including bioimaging assays.

QDs have dimensions between 1 and 100 nm and show an electronic energy states distribution between that of a discrete molecule and of the bulk semiconductor which are characterized by a bandgap energy (E_g)—the minimum energy required to excite an electron from the ground state valence energy band into the vacant conduction energy band. When an electron on the ground state valence band absorbs energy greater than E_g it is excited into the conduction energy band originating an exciton that emits photon (radiative recombination). CDs are constituted mainly by carbon with sp^2 hybridization characteristic of monocristaline graphite with relatively high oxygen contents. Because graphitic carbon is not a semiconductor a fluorescent mechanism similar to QDs is not possible. Alternatively, a surface defects based luminescence mechanism is being suggested for CDs [14].

Molecular fluorescence is intrinsically a multidimensional technique and a spectrofluorometer is a second order

instrument [15]. Indeed, a fluorescence spectrophotometer has two monochromators and an emission spectrum can be obtained for all excitation wavelengths of a sample and a data matrix of fluorescence intensities is obtained as function of the excitation and emission wavelengths—the excitation emission matrix (EEM). Second order instruments are becoming common in the analytical chemistry laboratory and they have several advantages allowing robust and unbiased estimations of the concentrations of the analytes in the samples—the so called second order advantage [15–17].

The second order advantage is the basis of the success of the application of this new nanosensing approach to complex chemical/biological systems. Indeed, it will only be possible if chemometric data analysis techniques are coupled to the detection apparatus in order to make results more robust and reliable. Several studied have already been done to demonstrate the advantages of the chemometric processing of the fluorescent signals generate by nanomaterials [18–22].

One of the most versatile chemometric techniques that can deal with second order data structures is multivariate curve resolution with alternating least squares (MCR-ALS) [23–31]. The MCR-ALS model does not assume the trilinearity of the data. Beside this, and attending to the previous knowledge of the data, the application of constraints as non negativity, unimodality, closure, selectivity, trilinearity, shape, zero concentration windows and correspondence of species allows to improve the estimations found and enlarge the applicability of the model [23–26].

This paper presents the application of MCR-ALS to two EEM data sets corresponding to two nanosystems: the quenching of the fluorescence of carbon dots (CDs) by Hg (II) ion [10]; and, the effect of the ionic strength on the EEM of the nanocomposite constituted by CdS quantum dots (QDs) and the dendrimer DAB (CdS-DAB) [19].

Experimental

Synthesis of Nanocomposites

The synthesis of the carbon dots was performed by laser ablation [UV pulsed laser irradiation (248 nm, KrF)] of carbon targets immersed in deionized water and they were activated in 0.1 M nitric acid and NH_2-polyethylene glycol (PEG_{200}) and functionalized with N-acetyl-L-cysteine to make them sensible to Hg(II) ions [10–14]. The raw carbon nanoparticles are not fluorescent and in order to make particles fluorescent the oxidation of the surface carbons to carboxylic acid groups with nitric acid and capping the nanoparticle with PEG_{200} are necessary treatments [14].

The aqueous synthesis of the nanocomposite constituted by the DAB dendrimer and CdS quantum dots used a generation five DAB dendrimer (polypropylenimine tetrahexacontaamine dendrimer generation 5) dissolved in water followed by the sequential addition of cadmium chloride, mercaptoacetic acid and sodium sulfide (the nanocomposite solution was purified by dialysis and centrifugation) [19, 20].

Instrumentation

All EEM were obtained in a quartz cuvette with a Spex 3D luminescence spectrophotometer equipped with a Xenon pulse discharge lamp (75 W) and a CCD detector. The EEM were acquired with a resolution of 2 nm in the following conditions: CDs-Hg, excitation wavelength range between 200.5 and 675.1 nm, emission wavelength range between 200.7 and 718.7 nm, slits of 0.05 mm and 3 s integration time; and, CdS-DAB-IS, excitation wavelength range between 199.4 and 672.8 nm; emission wavelength range between 349.7 and 719.7 nm, slits of 0.25 mm and y integration time.

EEM Data Structures

Three-way data sets of EEMs [excitation (nm) × emission (nm) × experimental factor] of the CDs obtained at different Hg(II) concentration values and CdS-DAB QDs obtained at different ionic strength values were analyzed using the MCR-ALS model [10, 19].

The raw experimental EEM are reduced in order to isolate the fluorescence band and try to eliminate the non-linear first order Rayleigh scattering. The reduction done was: CDs—excitation wavelength range—276.6 to 390.8 nm (52 wavelengths) and emission wavelength range—427.4 to 583.5 nm (76 wavelengths); CdS-DAB QDs—excitation wavelength range—228.1 to 381.1 nm (70 wavelengths), emission wavelength range—427.4 to 583.5 nm (141 wavelengths). Figure 1 shows the raw and analysed CDs-Hg-EEMs and CdS-DAB-IS-EEMs at the data set where a maximum fluorescence intensity is observed.

MCR-ALS

For the three-way data analysis with MCR-ALS the EEMs data sets are structured as [(Hg concentration (M) × emission (nm)) × excitation (nm)] for the CDs EEMs or [(ionic strength × emission (nm)) × excitation (nm)] for the QDs CdS-DAB EEMs.

The MCR-ALS estimations are found by an iterative alternating least squares procedure. As convergence criteria, given in percentage of change of standard deviation of residuals between two consecutive iterations, a value of 0.1% and a maximum number of iterations 200 were used. The initial estimates used for the three models were the estimates of a model without constraints. The non-negativity constraints are applied in all the dimensions of the EEMs. Beside this constraint the trilinearity constraint was also applied in one

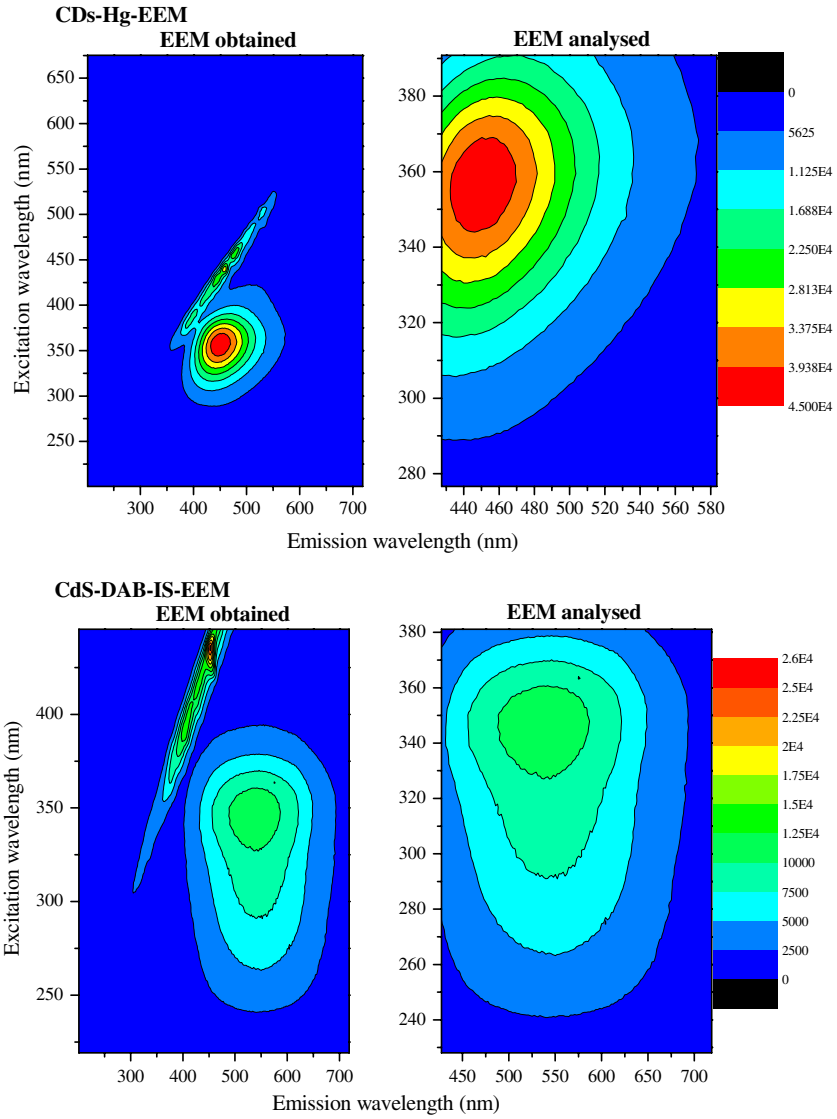

Fig. 1 Raw and analysed EEMs at the data set where a maximum fluorescence intensity is observed

component (principal fluorescent component) or in all components. The MCR-ALS decomposition of a three-dimensional structure $\underline{\mathbf{X}}(I \times J \times K)$ follow the mathematical formulation shown in Eq. 1 and is obtained through the augmentation of the K individual EEM data matrices simultaneous analyzed. In this equation the matrix $\mathbf{E}_k$ holds the residuals.

$$\mathbf{X}_k = \mathbf{C}_k\mathbf{S}^T + \mathbf{E}_k, k = 1, \ldots, K \tag{1}$$

In the MCR-ALS model (1) the X_k ($L \times J$), with L equal to ($I \times K$), is the augmented data matrix, $\mathbf{C}_k$ ($L \times F$) is the first-mode loading matrix and $\mathbf{S}$ ($J \times F$) is the loading matrix of the second mode. The third mode loading is contained in the $\mathbf{C}_k$ first mode loading.

Error Analysis

The results obtained from the MCR-ALS three-way data analysis were compared using the model fit [Fit (%)] and the percent of variation explained [R^2] respectively defined by Eq. 2 and 3 [32].

$$\text{Fit}(\%) = 100 \times \left(1 - \sqrt{\frac{\sum_{l=1}^{L}\sum_{j=1}^{J}(x_{lj} - \hat{x}_{lj})^2}{\sum_{l=1}^{L}\sum_{j=1}^{J}(x_{lj})^2}}\right) \tag{2}$$

$$R^2 = \frac{\sum_{l=1}^{L}\sum_{j=1}^{J}(x_{lj})^2 - \sum_{l=1}^{L}\sum_{j=1}^{J}(x_{lj} - \hat{x}_{lj})^2}{\sum_{l=1}^{L}\sum_{j=1}^{J}(x_{lj})^2} \tag{3}$$

In these equations $\hat{x}_{lj}$ is the lj element of the estimated bidimensional column-wise augmented data matrix and x_{lj} is the lj element of the experimental bidimensional column-wise augmented data matrix with $l = k \times i$.

The results obtained with MCR-ALS models were assessed using the lack of fit [LOF(%)] of the MCR-ALS model defined by Eq. 4 [32].

$$\mathrm{LOF}(\%) = 100 \times \left(\sqrt{\frac{\sum_{l=1}^{L}\sum_{j=1}^{J}(x_{lj} - \widehat{x}_{lj})^2}{\sum_{l=1}^{L}\sum_{j=1}^{J}(x_{lj})^2}} \right) \quad (4)$$

In this equation $\widehat{x}_{lj}$ is the lj element of the estimated bidimensional column-wise augmented data matrix by the MCR-ALS model and x_{lj} is the lj element of the experimental column-wise augmented data matrix in the $\mathrm{LOF}_{\mathrm{MCR\ vs\ Exp}}$ calculus and of the estimated with principal component analysis in the $\mathrm{LOF}_{\mathrm{MCR\ vs\ PCA}}$ calculation.

Software

The chemometric analysis was done in MATLAB® version 5.3. The algorithms for implementation of the MCR-ALS model were obtained from R. Tauler in http://www.mcrals.info/. All the graphs were done in Microcal Origin® version 7.5.

Results and Discussion

Preliminary Analysis of the Nanocomposites Data Structures

Figure 1 shows EEM of the raw nanocomposites and the excitation and emission wavelengths at maximum fluorescence intensity are 357.2 nm and 450.3 nm, for CDs-Hg-EEMs, and of 354.5 nm and 531.4 nm, for CdS-DAB-IS-EEMs.

The effect of increasing the Hg(II) concentrations on the EEM of CDs-Hg-EEMs was to provoke a decrease on the fluorescence intensity (quenching) and no wavelength shift was observed. This fluorescence quenching is due to the formation of quite stable complexes (static quenching) between the NAC residues on the surface of the CDs and Hg(II) resulting in charge transfer or heavy atom effects.

For the CdS-DAB-IS-EEMs, the increase of the ionic strength induces a smaller variation of the excitation wavelength (347.9 nm→367.8 nm) and a major variation of the emission wavelength (485.7 nm→633.4 nm) at maximum fluorescence intensity. This behaviour of the EEM of the CdS-DAB-IS-EEMs clearly shows a marked deviation of the trilinearity of the data structures.

In order to check for possible non-linearity and/or colinearity in the two sets of EEMs the SVD analysis of single and augmented row-wise matrices were performed. Figure 2 presents the normalized singular values for the single and augmented row-wise matrices. The SVD analysis (Fig. 2a) shows that for the CDs-Hg-EEMs augmented row-wise matrices of excitation and emission requires a greater number of components than the Hg(II) concentration. The SVD analysis (Fig. 2b) of the CdS-DAB-IS-EEMs augmented row-wise matrices of emission and ionic strength requires a greater number of components than the excitation. Attending to the previous knowledge of the data it is possible to conclude that the rank difference by SVD analysis suggests for the CDs-Hg-EEMs the existence of collinearity (rank deficiency) due to the possibility of a similar Hg concentration profile at different excitation and emission spectra (as previously observed by parallel factor

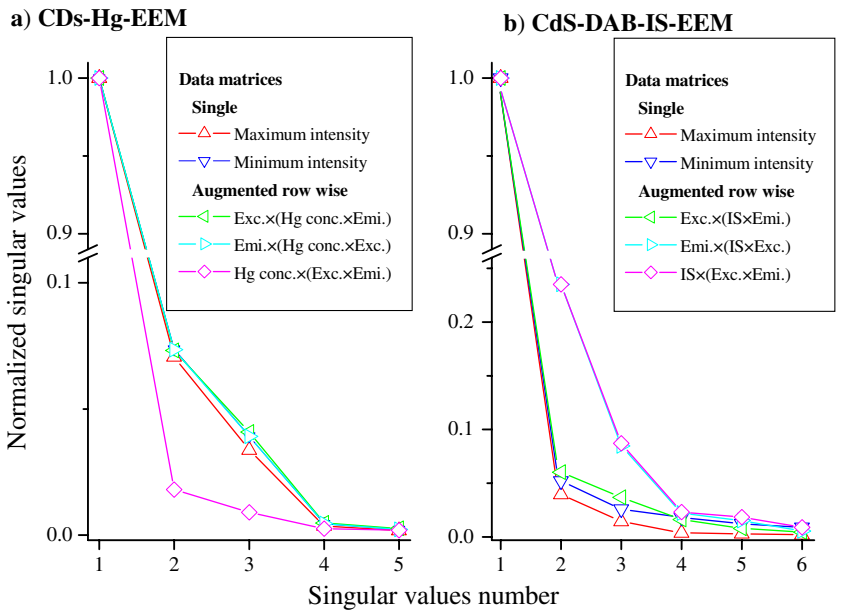

Fig. 2 Singular value decomposition of the singular data matrices and row-wise augmented data matrices in the excitation, emission and Hg or IS orders respectively in the analysis of the CDs-Hg-EEMs (**a**) and CdS-DAB-IS-EEMs (**b**)

analysis of these data structures [20]) and for the CdS-DAB-IS-EEMs the existence of non-linearity due to the shift of the excitation and emission wavelength at maximum fluorescence intensity.

This preliminary analysis clearly shows that the nanocomposites when subjected to chemical reactions and/or physical transformations cannot be described as one-component model (pure systems) and the corresponding multidimensional fluorescence data must be interpreted using multicomponent models. This observation is particularly critical when the nanomaterials are to be used as nanosensors, usually in complex systems such as for example in bioimaging [33]. In order to fully explore the nanomaterials under research, to obtain the photophysical characteristics of the different components and to develop a model for the nanosensor application a multicomponent self-modelling approach, such as MCR-ALS, should be used.

MCR-ALS Analysis

The right number of components that compose the experimental EEM data sets acquired as function of the experimental factors [Hg(II) concentration and ionic strength] were evaluated by MCR-ALS analysis using different component non negativity constraint models (from two and up to six components) (Table 1).

CDs-Hg-EEMs Nanocomposite System

The analysis of Table 1 shows that a three or a four components model adequately fit the CDs-Hg-EEMs three-way data structures—the fit is about 99% and R^2 is 0.9999. Figure 3 shows the estimations found with these two models using a non negativity constrained MCR-ALS.

The analysis of Fig. 3 shows the presence in the first and second dimensions of spectra compatible with fluorescence measurements (signal or background) and in the third dimension the intensity profiles as function of Hg(II) concentration. The analysis of the intensity profiles is most important because the quenching of the EEM was observed and, consequently, components with decreasing intensity profiles contain the analytical relevant information.

With the three component model only one component show a quenching profile (the first component) while with the four component model two components show quenching profiles (the first and the fourth component). These quenching components contain the relevant information about the fluorescent nanocomposites and will be subject of further study. The other two components show increasing intensity trends or noisy oscillations. These two components correspond to background signals: the increasing trend is due to scattering resulting from the hydrolysis of Hg(II) as consequence of the increasing concentration; and, the noisy variation is due to a background. Even so, and for the two models, also the third component could be a component with a noisy quenching profile.

Even if the data are inherently trilinear small deviations of the trilinearity could be expected. If the experimental factor does not induce deviations to the trilinearity, the greatest deviations to the trilinearity could be found in the components with the lowest fluorescence intensity or in the components corresponding to the background signal. So for a further analyse of the

Table 1 MCR-ALS non negativity constraint model evaluation in the analysis of the EEMs three way data structures

MCR-ALS					
	Number of components				
	Two	Three	Four	Five	Six
CDs-Hg-EEMs					
Fit (%)	95.83	99.14	99.28	99.33	99.35
R^2	0.9983	0.9999	0.9999	1.0000	1.0000
Number of iterations	200	200	96	200	100
Sum square of residuals	2.53×10^{10}	1.10×10^{9}	7.72×10^{8}	6.66×10^{8}	6.16×10^{8}
$LOF_{MCR\ vs.PCA}$ (%)	0.02	0.02	0.02	0.08	0.17
$LOF_{MCR\ vs\ Exp.}$ (%)	4.17	0.86	0.72	0.67	0.65
CdS-DAB-IS-EEMs					
Fit (%)	95.78	97.90	98.68	98.92	98.98
R^2	0.9982	0.9996	0.9998	0.9999	0.9999
Number of iterations	200	200	200	200	149
Sum square of residuals	3.12×10^{9}	7.68×10^{8}	3.07×10^{8}	2.03×10^{8}	1.82×10^{8}
$LOF_{MCR\ vs.PCA}$ (%)	1.71×10^{-3}	5.88×10^{-3}	0.08	0.24	0.37
$LOF_{MCR\ vs\ Exp.}$ (%)	4.23	2.10	1.33	1.08	1.02

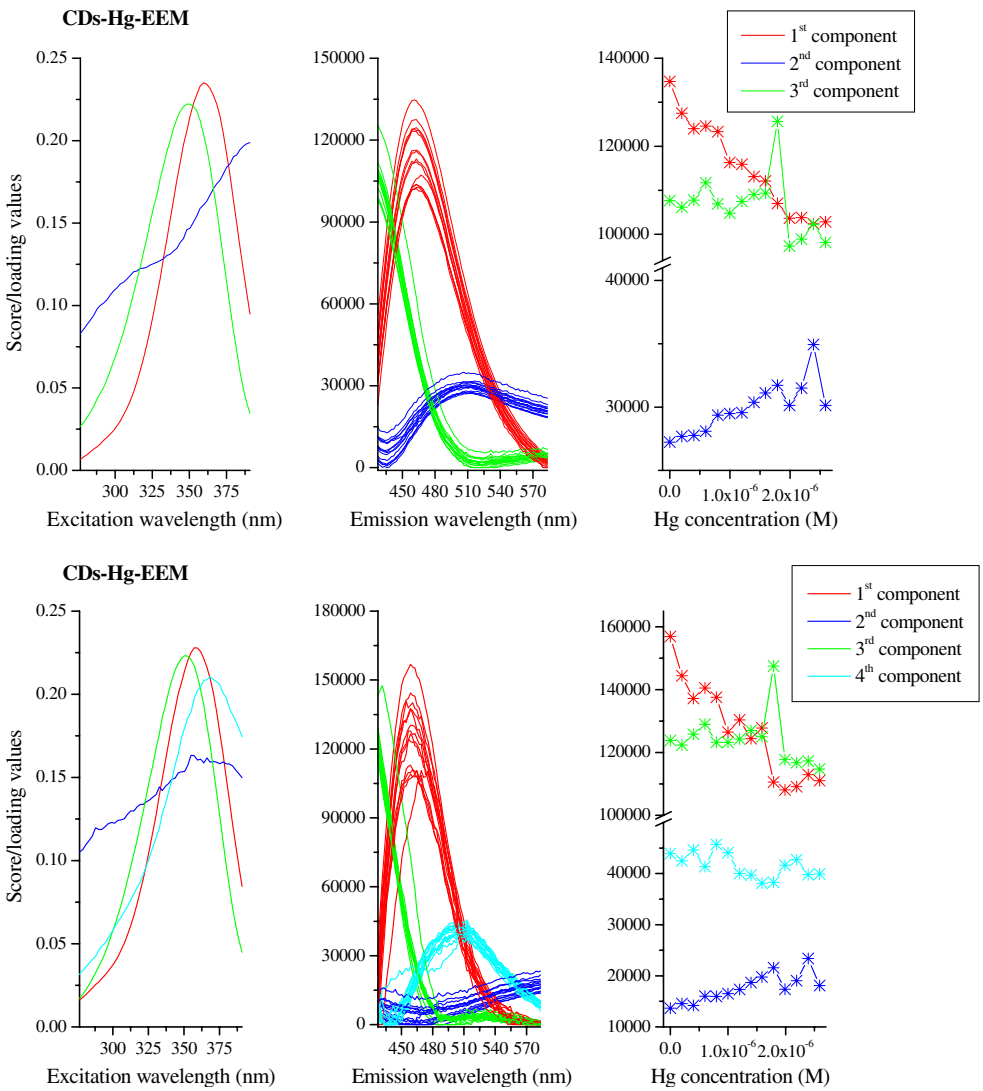

Fig. 3 Excitation spectra, emission spectra and experimental factor profile calculated with a MCR-ALS three and four components non-negativity constraint model in the analysis of the CDs-Hg-EEMs

intrinsic structure of the CDs-Hg-EEMs, and in particular the quenching components, the trilinear restriction was used in the first component and in all components of the three and four components models.

Table 2 presents the results found in this analysis and it shows that better fit parameters, with the exception of the number of iterations, is observed for the three components models. If a data structure is trilinear minor variations in the

Table 2 MCR-ALS non negativity and trilinearity constraint model evaluation in the analysis of the CDs-Hg-EEMs three way data structures

MCR-ALS				
	Number of components			
	Three - Non negativity	Four	Three - Non negativity	Four
	- Trilinearity in principal component		- Trilinearity in all components	
Fit (%)	98.87	98.40	98.73	98.30
R^2	0.9999	0.9997	0.9998	0.9997
Iterations	200	37	85	46
Sum square of residuals	1.89×10^9	3.77×10^9	2.38×10^9	4.28×10^9
$LOF_{MCR\ vs.PCA}$ (%)	0.73	1.43	0.93	1.82
$LOF_{MCR\ vs\ Exp.}$ (%)	1.13	1.60	1.27	1.96

model fit will be found when the trilinearity constraint is used. In comparison with the results found for the non negativity constraint models (Table 1) it is also possible to see that for the trilinearity constraint models a similar model fit is found for the three components and a lowest model fit is found for the four components.

Figures 4 and 5 show the estimations obtained respectively by a MCR-ALS non negativity and trilinearity constraint in the principal component and non negativity and trilinearity constraint in all the components. In the emission spectra dimension and for the components in which the trilinearity is applied only the first estimation, at maximum fluorescent intensity, is shown. Better estimations were found with three components trilinearity constraint model in all the components. For this model the first and third components correspond to CDs nanoparticles with different excitation spectrum, emission spectrum and Hg(II) concentration profile—a clear quenching profile for the first component and a quite noisy quenching profile for the third component. Also for this model, in comparison with the non negativity and trilinearity constraint model in the principal component, a greater variation of the Hg(II) concentration profile is observed. With the four components trilinearity constraint model in the principal and in all the components worse estimations are found in the excitation spectrum dimension. In this dimension two of the components correspond to the background signals.

The fact that MCR-ALS confirm that the CDs-Hg-EEM structure is trilinear is quite important from the analytical chemistry point of view. Indeed, this result shows that the nanocomposite fluorescent variations are only due to quenching and calibration can be achieved by modelling the quenching profiles of the components with the Stern-Volmer equation [10–12, 19–21, 29–31].

The analysis of the quenching profiles of the first and fourth components of the four component model show that they are similar but have different excitation and

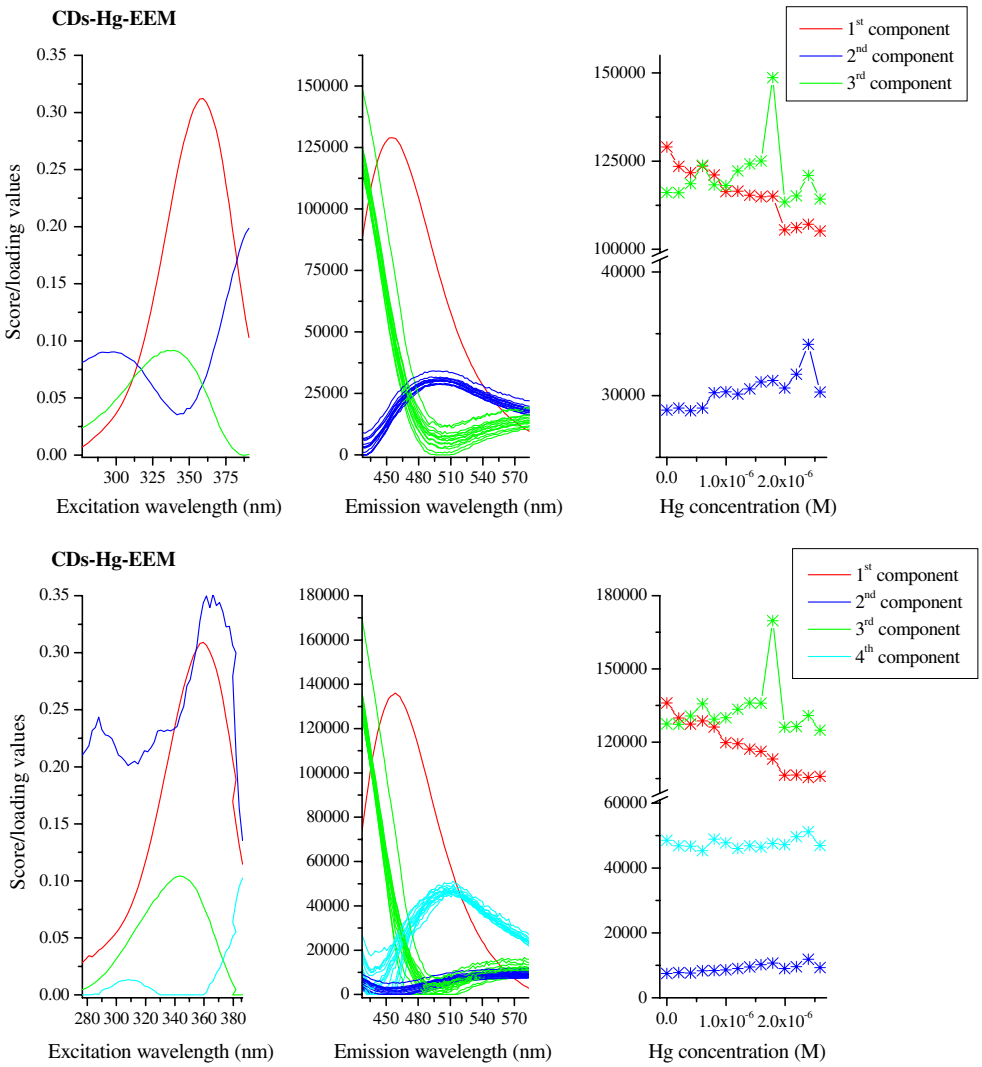

Fig. 4 Excitation spectra, emission spectra and Hg concentrationr profile calculated with a MCR-ALS three and four components non-negativity and trilinearity in the principal component constraint model in the analysis of the CDs-Hg-EEMs

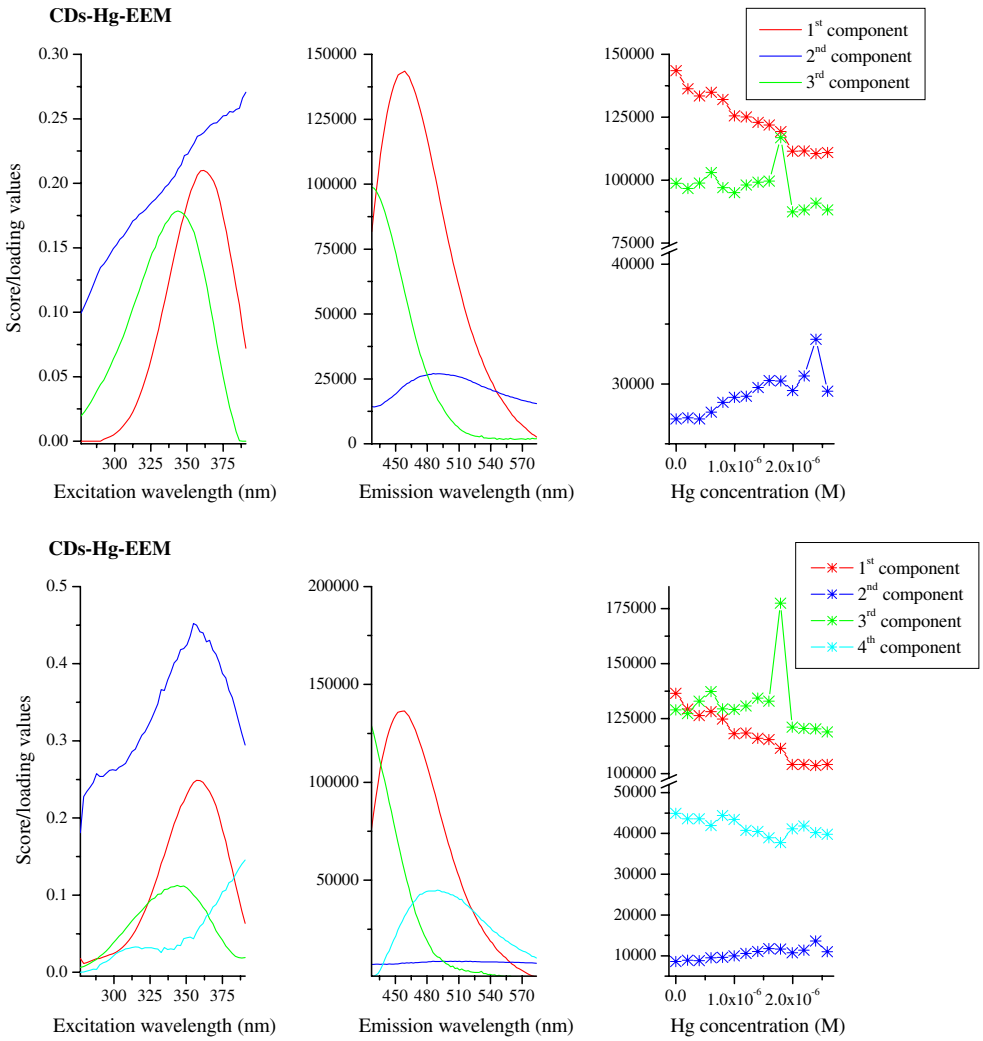

Fig. 5 Excitation spectra, emission spectra and experimental factor profile calculated with a MCR-ALS three and four components non-negativity and trilinearity in all the components constraint model in the analysis of the CDs-Hg-EEMs

emission spectra. This result show that the functionalised carbon dots are composed by at least two classes of nanoparticles that possesses similar affinity towards Hg (II). These two classes should correspond to two different size nanomaterials with the following maximum excitation and emission wavelengths: 360.6 and 458.4 nm; 343.8 and 428.2 nm. From the point of view of the synthetic nanotechnology of carbon dots this result is quite remarkable and can only be easily achieved using chemometric techniques of analysis of the EEM.

CdS-DAB-IS-EEMs System

The analysis of Table 1 shows that a four components model adequately fit the CdS-DAB-IS-EEMs three-way data structures—the fit is about 99% and R^2 is 0.9998 (the $LOF_{MCR\ vs\ Exp}$ and $LOF_{MCR\ vs\ PCA}$ values also confirm this number of components). Figure 6 shows the estimations calculated by the four components model with non negativity constraint plus, for comparison, the results obtained with the three components model. The different estimations obtained in the three dimensions for three and four components models clearly shows that a non trilinear CdS-DAB-IS-EEMs three-way data structure exists.

The analysis of the calculated spectra and fluorescence intensity profiles of the three dimensions show that three components correspond to the variations of the nanocomposite fluorescence with the ionic strength and one component corresponds to a background. The most important variation that is induced by the ionic strength is described by the first component with an excitation maximum at about 340 nm and with the following variation in the emission band: at lower ionic strengths the maximum of the emission band is at about 480 nm and with an increase of the ionic strength its intensity increase up to a concentration when a red shift is observed together with a decrease of the fluorescence intensity. Probably at higher ionic strengths values the aggregation of the nanoparticles is induced resulting in the expected red shift because the quantum confinement is reduced.

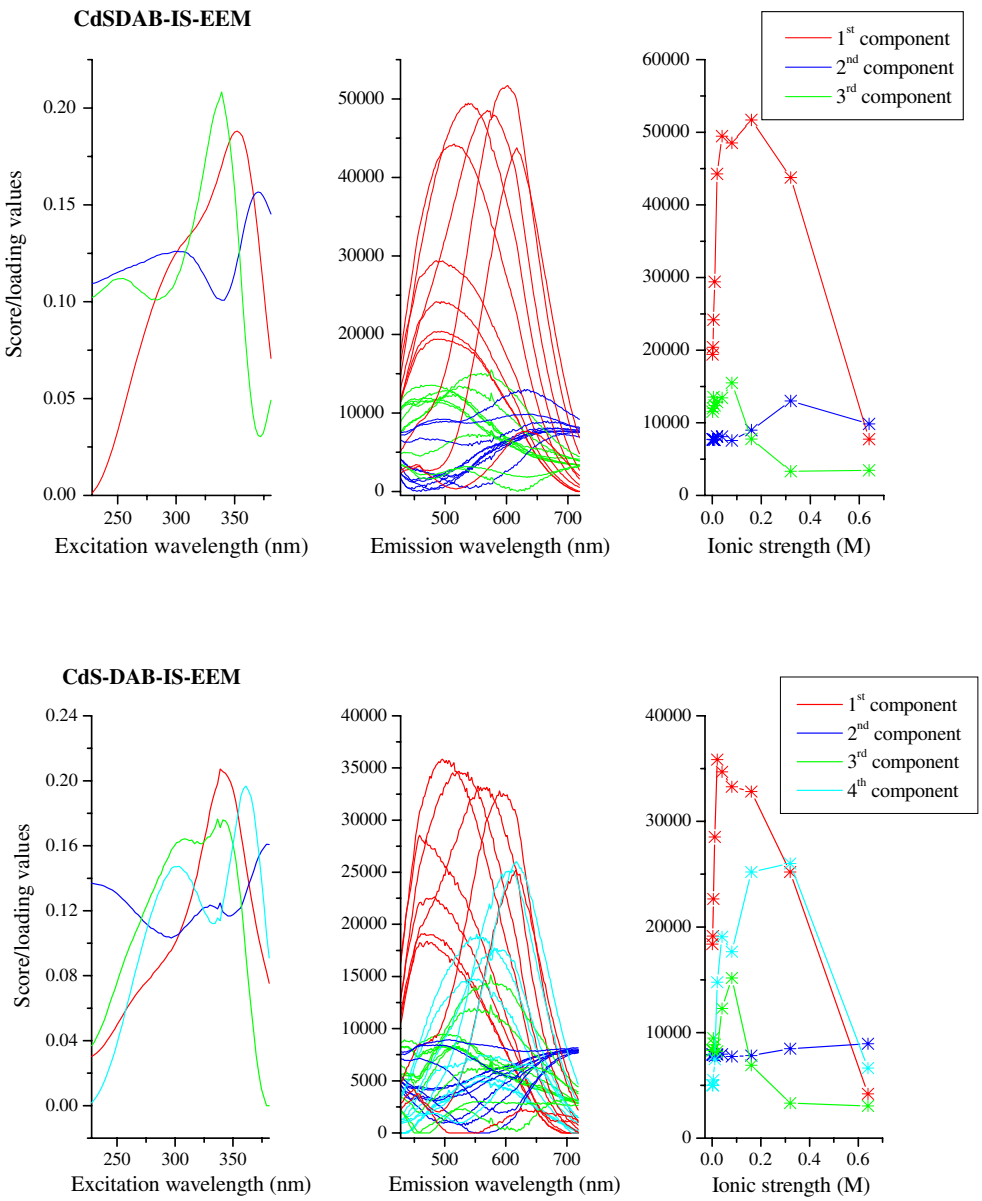

Fig. 6 Excitation spectra, emission spectra and experimental factor profile calculated with a MCR-ALS three and four components non-negativity constraint model in the analysis of the CdS-DAB-IS-EEMs

Conclusions

This paper reported the analysis of the response of two fluorescent nanomaterials that show potential as nanosensors for Hg(II) and ionic strength. The response of the nanosensors are characterized by EEM which allowed the use of multivariate chemometric techniques and using the second order advantage to fully explored the structure of the response data matrices. Quite surprisingly, in the two nanocomposites system under investigation, several linear independent response components were detected. This result suggests that if a lower dimension fluorescence technique is used the overall response of the nanosensors is not pure but composed by a mixture of several sources which could limit the quality of the analytical methodologies.

The self-modelling multivariate curve resolution used in this study, MCR-ALS, proved to be a quite versatile technique. Indeed, this technique successfully decomposed collinear components resulting from different sized carbon dots that respond similarly to the analyte and successfully modelled the non-linear response of the nanocomposite constituted by a dendrimer conjugated with quantum dots for different ionic strengths.

The size of the fluorescent nanomaterial is its most characteristic property because the fluorescence properties are size dependable. Usually nanosensors are constituted by mixtures of more or less similar sizes and, as shown in this paper, the overall sensor response is not pure. Consequently, in order to improve new nanosensor analytical methodologies it is recommended that a preliminary analysis of the fluorescence response

is done using multidimensional analytical responses (for example EEM) together with multivariate chemometric curve resolution techniques.

Acknowledgments Financial support from Fundação para a Ciência e a Tecnologia (FCT, Lisbon) (Programa Operacional Temático Factores de Competitividade (COMPETE) e comparticipado pelo Comunitário Europeu FEDER) (Project PTDC/QUI/71001/2006) is ackowledged.

References

1. Roduner E (2006) Size matters: why nanomaterials are different. Chem Soc Rev 35:583–592
2. Smith AM, Shuming N (2010) Semiconductor nanocrystals: structure, properties, and band gap engineering. Acc Chem Res 43:190–200
3. Regulacio MD, Han MY (2010) Composition-tunable alloyed semiconductor nanocrystals. Acc Chem Res 43:621–630
4. Han C, Li H (2010) Host-molecule-coated quantum dots as fluorescent sensors. Anal Bioanal Chem 397:1437–1444
5. Wang C, Gao X, Su X (2010) In vitro and in vivo imaging with quantum dots. Anal Bioanal Chem 397:1397–1415
6. Aswathy RG, Yoshida Y, Maekawa T, Kumar DS (2010) Near-infrared quantum dots for deep tissue imaging. Anal Bioanal Chem 397:1417–1435
7. Sun YP, Zhou B, Lin Y, Wang W, Fernando KAS, Pathak P, Meziani MJ, Harruff BA, Wang X, Wang HF, Luo PG, Yang H, Kose ME, Chen B, Veca LM, Xie SY (2006) Quantum-sized carbon dots for bright and colorful photoluminescence. J Am Chem Soc 128:7756–7757
8. Mao XJ, Zheng HZ, Long YJ, Du J, Hao JY, Wang LL, Zhou DB (2009) Study on the fluorescence characteristics of carbon dots. Spectroc Acta A 75:553–557
9. Yang ST, Cao L, Luo PG, Lu F, Wang X, Wang H, Mezian MJ, Liu G, Qi G, Sun YP (2009) Carbon dots for optical imaging in vivo. J Am Chem Soc 131:11308–11309
10. Gonçalves H, Jorge PAS, Fernandes JRA, Esteves da Silva JCG (2010) Hg(II) sensing based on functionalized carbon dots obtained by direct laser ablation. Sens Act B 145:702–707
11. Gonçalves H, Esteves da Silva JCG (2010) Fluorescent carbon dots capped with PEG200 and mercaptosuccinic acid. J Fluor 20:1023–1028
12. Gonçalves H, Duarte AJ, Esteves da Silva JCG (2010) Fiber optics carbon dots based mercury(II) sensor. Biosens Bioelectron 26:1302–1306
13. Zhang Y, Gonçalves H, Esteves da Silva JCG, Geddes CD (2011) Metal-enhanced photoluminescence from carbon nanodots. Chem Commun 47:5313–5315
14. Esteves da Silva JCG, Gonçalves H (2011) Analytical and bioanalytical applications of carbon dots. Trac - Trend Anal Chem Accepted
15. Books KS, Kowalski BR (1994) Theory of analytical chemistry. Anal Chem 66:782A–791A
16. Smilde A, Bro R, Geladi P (2004) Multi-way analysis: Applications in chemical sciences. Wiley, Chichester
17. Leitão JMM, Esteves da Silva JCG (2010) Fluorescence derivatization reaction and quantification of the antihypertensor Nifedipine. Global J Anal Chem 1:44–58
18. Leitão JMM, Gonçalves H, Mendonça C, Esteves da Silva JCG (2008) Multiway chemometric decomposition of EEM of fluorescence of CdTe quantum dots obtained as function of pH. Anal Chim Acta 628:143–154
19. Campos BB, Algarra M, Alonso B, Casado CM, Esteves da Silva JCG (2009) Mercury(II) sensing based on the quenching of fluorescence of CdS-dendrimer nanocomposites. Analyst 134:2447–2452
20. Campos BB, Algarra M, Esteves da Silva JCG (2010) Fluorescent properties of a hybrid cadmium sulfide-dendrimer nanocomposite and its quenching with nitromethane. J Fluor 20:143–151
21. Gonçalves H, Mendonça C, Esteves da Silva JCG (2009) PARAFAC analysis of the quenching of EEM of fluorescence of glutathione capped CdTe quantum dots by Pb(II). J Fluor 19:141–149
22. Leitão JMM, Gonçalves H, Esteves da Silva JCG (2010) Parallel factor analysis of EEM of the fluorescence of carbon dots nanoparticles. J Chemom 24:655–664
23. Tauler R (1995) Multivariate curve resolution applied to second order data. Chemom Intell Lab Syst 30:133–146
24. Juan A, Tauler R (1995) Comparison of three-way resolution methods for non-trilinear chemical data sets. J Chemom 15:749–772
25. Tauler R, Smilde A, Kowalski B (1995) Selectivity, local rank, three-way data analysis and ambiguity in multivariate curve resolution. J Chemom 9:31–58
26. Tauler R, Marqués I, Casassas E (1998) Multivariate curve resolution applied to three-way trilinear data: Study of a spectrofluorimetric acid–base titration of salicylic acid at three excitation wavelengths. J Chemom 12:55–75
27. Smilde AK, Tauler R, Saurina J, Bro R (1999) Calibration methods for complex second-order data. Anal Chim Acta 398:237–251
28. Antunes MCG, Pereira CCC, Esteves da Silva JCG (2007) MCR of the quenching of the EEM of fluorescence of humic substances by metal ions. Anal Chim Acta 595:9–18
29. Esteves Da Silva JCG, Tauler R (2006) Multivariate curve resolution of synchronous fluorescence spectra matrices of fulvic acids obtained as function of the pH. Appl Spectrosc 60:1315–1321
30. Esteves da Silva JCG, Tavares MJCG, Tauler R (2006) Multivariate curve resolution of multidimensional excitation-emission quenching matrices of a Laurentian soil fulvic acid. Chemosphere 64:1939–1948
31. Antunes MCG, Esteves da Silva JCG (2005) Multivariate curve resolution of multidimensional excitation-emission quenching matrices of a Laurentian soil fulvic acid. Anal Chim Acta 546:52–59
32. Jaumot J, Gargallo R, Juan A, Tauler R (2005) A graphical user-friendly interface for MCR-ALS: a new tool for multivariate curve resolution in MATLAB. Chemom Intell Lab Syst 76:101–110
33. Esteves da Silva JCG, Leitão JMM (2010) Parallel factor analysis methods and the second order advantage in molecular fluorescence analysis. Global J Anal Chem 1:161–168